AIAA JOURNAL
Vol. 36, No. 1, January 1998

Positivity Preservation and Adaptive Solution for the k–ϵ Model of Turbulence

Florin Ilinca*
National Research Council, Boucherville, Québec J4B 6Y4, Canada
and
Dominique Pelletier†
École Polytechnique de Montréal, Montréal, Québec H3C 3A7, Canada

A simple change of dependent variables that guarantees positivity of turbulence variables in numerical simulation codes is presented. The approach consists of solving for the natural logarithm of the turbulence variables, which are known to be strictly positive. The approach is valid for any numerical scheme, be it a finite difference, a finite volume, or a finite element method. The work focuses on the advantages of the proposed change of dependent variables within the framework of an adaptive finite element method. The turbulence equations in logarithmic variables are presented for the standard k–ϵ model. Error estimation and mesh adaptation procedures are described. The formulation is validated on a shear layer case for which an analytical solution is available. This provides a framework for rigorous comparison of the proposed approach with the standard solution technique, which makes use of k and ϵ as dependent variables. The approach is then applied to solve turbulent flow over a NACA0012 airfoil for which experimental measurements are available. The proposed procedure results in a robust adaptive algorithm. Improved predictions of turbulence variables are obtained using the proposed formulation.

Nomenclature

E	= roughness parameter
$\mathcal{E}$	= natural logarithm of the turbulent dissipation rate
$\boldsymbol{f}$	= body force
h	= element size
$\mathcal{K}$	= natural logarithm of the turbulent kinetic energy (TKE)
k	= TKE
Pe	= Péclet number
$P(\boldsymbol{u})$	= production term
p	= pressure
q	= solution derivative
$\mathcal{R}$	= equation residual
$\boldsymbol{u}$	= velocity vector
ϵ	= turbulent dissipation rate
κ	= von Kármán constant
μ	= viscosity
ρ	= density
τ	= stabilization parameter
τ_w	= wall shear stress
∇	= gradient operator
$\nabla\cdot$	= divergence

Subscripts

ex	= exact solution
h	= finite element solution
T	= turbulent
w	= values on the boundary

I. Introduction

ADAPTIVE finite element methods provide a powerful approach for tackling complex computational fluid dynamics problems. They provide accurate solutions at a reasonable cost by automatically clustering elements around flow features of interest such as shear layers, boundary layers, and reattachment points. The adaptive process is also cost effective in the sense that the best numerical solution is obtained at the least computational cost. However, one major hurdle in the numerical simulation of turbulent flows using two-equation models lies in ensuring that the turbulence variables (k and ϵ) remain positive throughout the flow domain and during the course of iterations. Failure to ensure this realizability condition can have devastating effects on the solution process. The eddy viscosity may locally become negative and result in immediate and irrecoverable breakdown of iterations.

Various approaches have been devised to deal with this problem, ranging from the implementation of clipping operators or limiters,[1–3] the design of special upwind finite volume schemes,[4,5] and the use of discretization schemes that help preserve positivity (linearization and implicit treatment of source terms)[5,6] to the design of turbulence models less prone to this kind of breakdown.[7,8] The last approach presents the drawback of possibly imposing limitations on the turbulence modeling effort with the result that some potentially useful mathematical model might be discarded because the numerical scheme cannot handle it properly. Upwind schemes have shown good potential in finite volume algorithms. However, upwind schemes cannot guarantee positivity under all circumstances. Positivity promoting algorithms are usually designed on a case by case basis because their structure depends in part on the turbulence model that has been retained. Use of solution clipping and limiters is very widespread. It is a very robust approach in the sense that positivity can be enforced at every time step or every iteration and that it can be applied to almost any numerical algorithm to solve the Reynolds-averaged Navier–Stokes equations. However, it does have two drawbacks. First, it slows down the convergence of the iterative solver because clipped values of the solution destroy the residuals of the solution. Second, clipping introduces noises and oscillations in the solution fields. Negative values that are locally reset to some small positive values can result in locally very large solution gradients and, hence, large curvature, even if the values of k and ϵ are small. This is extremely detrimental to adaptive solution algorithms because they tend to cluster grid points in these regions. The net result is that the mesh is being adapted to the inability of the solver to produce a smooth and positive solution rather than refining the grid in regions of large solution curvature.

Thus, there is a need to improve the quality of the flow solver to benefit fully from the potential offered by adaptive methods. This paper presents a change of dependent variables for turbulence quantities that results in improved solution quality (smoothness) so

Received Dec. 13, 1996; revision received May 23, 1997; accepted for publication Sept. 6, 1997.

*Postdoctoral Fellow, Industrial Materials Institute, 75, de Mortagne. Member AIAA.

†Professor, Department of Mechanical Engineering, P.O. Box 6079, Succursale Centre-ville. Associate Fellow AIAA.

that quantitative improvements by adaptive remeshing can be fully realized. The computational variables are the natural logarithm of k and ϵ. This choice has several important advantages. The eddy viscosity, k, ϵ, and the source terms in the turbulence equations are now obtained as the exponential of the computational dependent variables. Hence, these terms are all strictly positive throughout the domain. Furthermore, it is a well-known property of the logarithm that it varies more slowly than its argument. This results in improved accuracy in regions of rapid variation of the turbulence fields such as boundary layers, stagnation points, and shear layers. The cost incurred for these benefits is a mild increase of the nonlinearity of the system of partial differential equations to be solved.

The paper is organized as follows. Section II presents the Reynolds-averaged Navier–Stokes equations and the turbulence equations for the standard k–ϵ model. Section III discusses the change of variables leading to the logarithmic variable form of the turbulence equations. The section discusses the advantages for using such variables. Section IV presents the finite element formulation for solving the transformed equations. Section V presents the error estimation and adaptive strategies used in conjunction with the new variables. Here again advantages of the new formulation with regard to error control and adaptivity are discussed: solution smoothness, eddy viscosity representation, and robustness in region of low turbulence. Section VI presents results obtained on problems for which a closed-form solution or experimental data are available. The paper closes with conclusions.

II. Modeling of the Problem

A. Reynolds-Averaged Navier–Stokes Equations

The flow regime of interest is modeled by the Reynolds-averaged Navier–Stokes equations

$$\rho \boldsymbol{u} \cdot \nabla \boldsymbol{u} = -\nabla p + \nabla \cdot \left[(\mu + \mu_T)(\nabla \boldsymbol{u} + \nabla \boldsymbol{u}^T)\right] + \rho \boldsymbol{f}$$

$$\nabla \cdot \boldsymbol{u} = 0$$

The turbulent viscosity μ_T is computed using the k–ϵ model of turbulence

$$\mu_T = \rho C_\mu (k^2/\epsilon)$$

The system is closed by including the transport equations for the turbulence quantities[9]:

$$\rho \boldsymbol{u} \cdot \nabla k = \nabla \cdot \{[\mu + (\mu_T/\sigma_k)]\nabla k\} + \mu_T P(\boldsymbol{u}) - \rho\epsilon$$

$$\rho \boldsymbol{u} \cdot \nabla \epsilon = \nabla \cdot \{[\mu + (\mu_T/\sigma_\epsilon)]\nabla \epsilon\} + C_{\epsilon 1}(\epsilon/k)\mu_T P(\boldsymbol{u}) - C_{\epsilon 2}\rho(\epsilon^2/k)$$

where the production of turbulence is defined as

$$P(\boldsymbol{u}) = \nabla \boldsymbol{u} : (\nabla \boldsymbol{u} + \nabla \boldsymbol{u}^T)$$

The constants σ_k, σ_ϵ, $C_{\epsilon 1}$, $C_{\epsilon 2}$, and C_μ take on the standard values proposed by Launder and Spalding.[9]

To increase the robustness of the finite element scheme, the equations for k and ϵ are rewritten by using the eddy viscosity definition.[10,11] Thus, ϵ may be rewritten as

$$\epsilon = \rho C_\mu (k^2/\mu_T)$$

to achieve the following block-triangular form of the turbulence equations:

$$\rho \boldsymbol{u} \cdot \nabla k = \nabla \cdot \{[\mu + (\mu_T/\sigma_k)]\nabla k\} + \mu_T P(\boldsymbol{u}) - \rho C_\mu \left(k^2/\mu_T\right)$$

$$\rho \boldsymbol{u} \cdot \nabla \epsilon = \nabla \cdot \{[\mu + (\mu_T/\sigma_\epsilon)]\nabla \epsilon\} + \rho C_{\epsilon 1} C_\mu k P(\boldsymbol{u}) - C_{\epsilon 2}\rho(\epsilon^2/k)$$

The equations can now be solved in the following order: momentum continuity, k, and then ϵ. Details on the iterative solution algorithm are given in Ref. 1.

B. Wall Boundary Conditions

On the boundary, a combination of Neumann and Dirichlet conditions is imposed using wall functions that describe the asymptotic behavior of the different variables near a solid wall.[9] For the turbulent kinetic energy we consider the normal gradient to the wall equal to zero,[12] and so the turbulent kinetic energy (TKE) values on boundary points k_w may be computed. Then we impose the wall shear stress given by

$$\tau_w = \frac{\rho U C_\mu^{\frac{1}{4}} k_w^{\frac{1}{2}}}{U^+}$$

where

$$U^+ = \begin{cases} y^+, & y^+ < y_c^+ \\ (1/\kappa)\ln(Ey^+), & y^+ \geq y_c^+ \end{cases}$$

$$y^+ = \frac{\rho C_\mu^{\frac{1}{4}} k_w^{\frac{1}{2}} y}{\mu}$$

where U is the norm of the velocity, y is the distance between the computational boundary and the wall, and E is a roughness parameter ($E = 9.0$ for smooth walls). Finally, the dissipation of the TKE on the boundary points is given by

$$\epsilon_w = \frac{C_\mu^{\frac{3}{4}} k_w^{\frac{3}{2}}}{\kappa y}$$

C. k–ϵ Finite Element Solver

The finite element equations for the original forms of the turbulence equations are obtained by multiplying the differential equations by suitable test functions and applying the divergence theorem to diffusion terms. This leads to the following Galerkin variational equations.

1) Momentum and continuity:

$$(\rho \boldsymbol{u} \cdot \nabla \boldsymbol{u}, \boldsymbol{v}) + a(\boldsymbol{u}, \boldsymbol{v}) - (p, \nabla \cdot \boldsymbol{v}) = (\rho \boldsymbol{f}, \boldsymbol{v}) + \langle t^*, \boldsymbol{v} \rangle$$

$$(q, \nabla \cdot \boldsymbol{u}) = 0$$

with

$$(h, g) = \int_V hg \, \mathrm{d}V$$

$$a(\boldsymbol{u}, \boldsymbol{v}) = \int_V (\mu + \mu_T)[\nabla \boldsymbol{u} + \nabla \boldsymbol{u}^T] : \nabla \boldsymbol{v} \, \mathrm{d}V$$

$$\langle t^*, \boldsymbol{v} \rangle = \int_{\partial K \setminus \Gamma_t} \left[(\mu + \mu_T)(\nabla \boldsymbol{u} + \nabla \boldsymbol{u}^T) \cdot \boldsymbol{n} - p\boldsymbol{n}\right] \cdot \boldsymbol{v} \, \mathrm{d}s + \int_{\partial K \cap \Gamma_t} \tau_w \cdot \boldsymbol{v} \, \mathrm{d}s$$

where $\partial K \setminus \Gamma_t$ denotes either a freestream or an outflow boundary and $\partial K \cap \Gamma_t$ represents the portion of the boundary where the law of the wall will be applied.

2) k equation:

$$\int_V \left[\rho \boldsymbol{u} \cdot \nabla k w + \left(\mu + \frac{\mu_T}{\sigma_k}\right)\nabla k \cdot \nabla w + \rho^2 C_\mu \frac{k^2}{\mu_T} w\right] \mathrm{d}V = \int_V \mu_T P(\boldsymbol{u}) w \, \mathrm{d}V$$

3) ϵ equation:

$$\int_V \left[\rho \boldsymbol{u} \cdot \nabla \epsilon s + \left(\mu + \frac{\mu_T}{\sigma_\epsilon}\right)\nabla \epsilon \cdot \nabla s + C_{\epsilon 2}\rho \frac{\epsilon^2}{k} s\right] \mathrm{d}V = \int_V C_{\epsilon 1} \rho C_\mu k P(\boldsymbol{u}) s \, \mathrm{d}V$$

The momentum and turbulence transport equations are dominated by convection, and it is well known that a standard Galerkin discretization leads to oscillations in the solutions. Hence, some form of upwinding is required to suppress these nonphysical oscillations. Here we use a Galerkin least-squares (GLS) method as described by Hughes et al.[13,14] In this approach we add to the standard Galerkin form of the equations, terms obtained from the minimization of the square of the equation's residuals.[15,16] Consequently, we minimize the functional

$$J = \sum_{e=1}^{n_{\text{elem}}} \int_{V^e} \left(\tau_u \mathcal{R}_u^2 + \tau_p \mathcal{R}_p^2 + \tau_k \mathcal{R}_k^2 + \tau_\epsilon \mathcal{R}_\epsilon^2\right) \mathrm{d}V^e$$

where $\mathcal{R}_u$, $\mathcal{R}_p$, $\mathcal{R}_k$, and $\mathcal{R}_\epsilon$, are, respectively, the residuals of the momentum, continuity, turbulent energy, and turbulent dissipation equations; and τ_u, τ_p, τ_k, and τ_ϵ are stabilization parameters. For the momentum, k, and ϵ equations, we define the parameter τ as[13]

$$\tau = \delta h/2|V|$$

where $|V|$ is the norm of the velocity and δ is a parameter depending on the local Péclet number:

$$\delta = \coth(Pe) - \frac{1}{Pe}, \qquad Pe = \frac{\rho h|V|}{2\lambda}$$

Here λ is the diffusion coefficient of the transport equation under consideration. For the continuity equation, the stabilization parameter is computed as[17]

$$\tau_p = h^2/2\tau_u$$

The additional GLS contributions are discontinuous across element faces; consequently, terms containing them will be integrated only on the element interiors. For more details, see Ref. 18. The equations are discretized using the seven-node triangular element, which uses an enriched quadratic velocity field, a linear discontinuous pressure, and a quadratic interpolant for turbulent variables.

D. Limiters for Turbulence Variables

The turbulence equations contain divisions by k, ϵ, and μ_T. Hence, negative or small values of the denominator can lead to improper sign or overly large values for μ_T or for some source terms. A negative value for the eddy viscosity always has catastrophic effects on the solution and the solver because it makes the equations hyperbolic. To enhance robustness of the algorithm, both k and ϵ are limited from below to prevent them from taking overly small values. If k is too small, it is replaced by $k = k_{\max}/d_k$, where $k_{\max}$ is the maximum value found in the domain and d_k is a user-supplied constant. If ϵ is too small and results in overly large values of μ_T, it is replaced by $\epsilon = \rho C_\mu(k^2/d_\mu\mu_l)$, where d_μ is a user-supplied constant establishing the lower bound of μ_T as μ_l. Here μ_l is the fluid viscosity. When quadratic interpolation functions are used, we might have positive nodal values for k and ϵ for which the solution become negative inside the element. Hence, turbulence variables must also be limited from below at integration points.[1,2]

III. Positivity Preserving Approaches

Although the aforementioned techniques provide a useful tool for solving turbulent flows, they do present a number of drawbacks. First, the iteration process is quite sensitive to the mesh. Most often, fairly fine meshes must be used to ensure that enough resolution is provided to obtain smooth solutions.[1,2] This can be quite expensive, especially in three dimensions. Second, the clipping process used to enforce positivity results in local oscillations in the turbulence fields. This is very detrimental to the adaptive process because the error estimation technique, described later in the paper, detects these ripples and mistakenly identifies them as regions requiring mesh refinement. The net result is that adaptation is most often wasted on wiggles generated by the solver rather than being applied to improve accuracy in regions of large solution curvature. Regions that do require mesh refinement may be overlooked, with the consequence that it is sometimes impossible to obtain a solution on the adapted mesh because the flow solver diverges. In other words, the mesh adaptation is being driven by deficiencies in the flow solver rather than by the flow physics.

The usual fix consists of designing an initial mesh that is sufficiently fine that ripples will be nearly absent, thus defeating the original purpose of the mesh adaptation process. Such symptoms are most clearly seen in free shear flows when both turbulence variables decrease asymptotically toward zero but at such rates that the eddy viscosity asymptotes to some small but constant value that often is several orders of magnitude larger than the turbulence variables themselves.[2] This phenomenon has been observed, for the case of internal flow over a backward-facing step, in the shear layer emanating from the step corner.[1] In this layer all turbulence variables, including the eddy viscosity, present very sharp fronts across which the variables decrease by several orders of magnitude to approach very small values. Wiggles on the side of small values can lead to negative k, ϵ, or eddy viscosity inside an element. Clipping is triggered in these region with the effect of introducing additional kinks in the solution. Clipping can also result in mesh refinement next to fronts rather than across them.

One way to preserve positivity of the dependent variables consists in solving for their logarithms.[18] This can be viewed as using the following change of dependent variables:

$$\mathcal{K} = \ell n(k), \qquad \mathcal{E} = \ell n(\epsilon)$$

Solving for $\mathcal{K}$ and $\mathcal{E}$ guarantees that the turbulence quantities of interest (namely, k and ϵ) will remain positive throughout the computations. Hence the eddy viscosity μ_T will always remain positive. We refer to this approach as solving for logarithmic variables. This approach presents another advantage. Any given field of a turbulence quantity presents very large variations of amplitude across very steep fronts that are difficult to resolve accurately. The fields of the logarithmic variables $\mathcal{K}$ and $\mathcal{E}$ present smoother variations than those of k and ϵ because the logarithm varies more slowly than its arguments. Hence, more accurate solutions can be expected when logarithmic variables are used. Examples shown later in the paper confirm this.

The turbulence model equations for logarithmic variables are as follows:

$$\rho\boldsymbol{u}\cdot\nabla\mathcal{K} = \nabla\cdot\{[\mu + (\mu_T/\sigma_k)]\nabla\mathcal{K}\} + [\mu + (\mu_T/\sigma_k)](\nabla\mathcal{K})^2 + \mu_T e^{-\mathcal{K}}P(\boldsymbol{u}) - \rho^2 C_\mu\left(e^{\mathcal{K}}/\mu_T\right)$$

$$\rho\boldsymbol{u}\cdot\nabla\mathcal{E} = \nabla\cdot\{[\mu + (\mu_T/\sigma_\epsilon)]\nabla\mathcal{E}\} + [\mu + (\mu_T/\sigma_\epsilon)](\nabla\mathcal{E})^2 + \rho C_{\epsilon_1} C_\mu e^{\mathcal{K}-\mathcal{E}}P(\boldsymbol{u}) - C_{\epsilon_2}\rho e^{\mathcal{E}-\mathcal{K}}$$

with the following definition for the eddy viscosity:

$$\mu_T = \rho C_\mu e^{2\mathcal{K}-\mathcal{E}}$$

Now all of the turbulence variables (k, ϵ, and μ_T) are discretized in the same way. They are computed as exponentials of the quadratic finite element solution. The production and dissipation terms also contain exponentials. Numerical integration is performed in the finite element formulation using a Gaussian quadrature rule with a large number of integration points (here a 16-points rule integrates exactly polynomials of degree up to 8).

Note that the use of logarithmic variables has removed the troublesome division by ϵ in the eddy viscosity and replaced it by a subtraction of arguments to the exponential function. Also, a number of other worrisome divisions have been removed from the differential equations for the turbulence variables. The price to pay for this advantage is the appearance of exponentials in the right-hand side of the turbulence equations. However, because k and ϵ take on small values, the exponential is very flat so that the nonlinearity is very mild. In fact, our experience indicates that the use of logarithmic variables significantly enhances convergence of the solver.

IV. Finite Element Formulation

The preceding form of the turbulence equations gives rise to the following Galerkin finite element formulation for the turbulence equations:

$$\int_V \left[\rho\boldsymbol{u}\cdot\nabla\mathcal{K}w + \left(\mu + \frac{\mu_T}{\sigma_k}\right)\nabla\mathcal{K}\cdot\nabla w - \left(\mu + \frac{\mu_T}{\sigma_k}\right)(\nabla\mathcal{K})^2 w + \rho^2 C_\mu\frac{e^{\mathcal{K}}}{\mu_T}w\right]\mathrm{d}V = \int_V \mu_T e^{-\mathcal{K}}P(\boldsymbol{u})w\,\mathrm{d}V$$

$$\int_V \left[\rho\boldsymbol{u}\cdot\nabla\mathcal{E}w + \left(\mu + \frac{\mu_T}{\sigma_\epsilon}\right)\nabla\mathcal{E}\cdot\nabla w - \left(\mu + \frac{\mu_T}{\sigma_\epsilon}\right)(\nabla\mathcal{E})^2 w + C_{\epsilon_2}\rho e^{\mathcal{E}-\mathcal{K}}w\right]\mathrm{d}V = \int_V \rho C_{\epsilon_1} C_\mu e^{\mathcal{K}-\mathcal{E}}P(\boldsymbol{u})w\,\mathrm{d}V$$

Here again we make use of a GLS method to obtain stable solutions to convection dominated problems. The GLS variational equations for logarithmic variables are presented in Ref. 18.

V. Adaptive Methodology

A. Error Estimation and Adaptive Remeshing

The adaptive remeshing procedure described by Ilinca et al.[11] and Ilinca[18] is used to cluster grid points in regions of rapid variations of all dependent variables: velocity, pressure, logarithmic turbulence variables, and the eddy viscosity. Error estimates are obtained by a local least-squares reconstruction of the solution derivatives.[19,20] In the case of the velocity field, the strain rate tensor is used for error estimation. An error estimate of the pressure solution is obtained by local projection of the pressure field itself. Error estimates are obtained for turbulence variables by projecting the finite element derivatives of $\mathcal{K}$ and $\mathcal{E}$ into a continuous field. Finally, an error estimate for the eddy viscosity is also constructed because slowly varying fields of $\mathcal{K}$ and $\mathcal{E}$ can result in rapid variation of the eddy viscosity. This is very important to the success of adaptation in turbulent flows because the eddy viscosity is the sole mechanism for transfer of momentum and turbulence kinetic energy by turbulent fluctuations. See Refs. 1, 2, and 10 for examples and some discussion of these issues. This approach was successfully applied by the authors to the k–ϵ model,[10] the k–ω model of turbulence,[21] turbulent heat transfer,[22] and a pressure-based finite element solution algorithm for compressible subsonic viscous flows.[23]

Once the error estimates are obtained for all variables, there remains the need to design a better mesh. The adaptive remeshing strategy is modeled after that proposed by Peraire et al.[24] In our approach all variables are analyzed and contribute to the mesh adaptation process. For this, an error estimation is made for each dependent variables independently. The mesh characteristics (element size) are derived for each variable on a given element. The minimum element size predicted by each of the dependent variables is selected on each element. Details of the steps of this algorithm are presented in Ref. 18.

B. Logarithmic Variables and Solution Errors

The effect of the change of variables on the solution accuracy can be best appreciated by looking at the relationship between the error in a given turbulence variable and the error in its natural logarithm. Let e_k and $e_{\mathcal{K}}$ denote the error in k and in its natural logarithm $\mathcal{K}$, respectively. We have the following relationships between the exact solution and its logarithm:

$$k_{\text{ex}} = e^{\mathcal{K}_{\text{ex}}}$$

We also have the following relationship between the exact values and their finite element approximation:

$$k_{\text{ex}} = k_h + e_k, \qquad \mathcal{K}_{\text{ex}} = \mathcal{K}_h + e_{\mathcal{K}}$$

We can then write

$$k_h + e_k = e^{\mathcal{K}_h + e_{\mathcal{K}}} = e^{\mathcal{K}_h} e^{e_{\mathcal{K}}} = e^{\mathcal{K}_h}\left[1 + e_{\mathcal{K}} + \mathcal{O}\left(e_{\mathcal{K}}^2\right)\right]$$

which, upon neglecting higher-order terms, leads to

$$k_h + e_k \approx k_h + k_h e_{\mathcal{K}}$$

That is

$$e_k \approx k_h e_{\mathcal{K}}$$

In other words, the error in the logarithm of k is proportional to the relative error in k. This observation plays a significant role for turbulent flows. Recall that the mesh adaptation strategy uses the principle of equidistribution of the error. Recall also that k is often very small in the freestream. With the use of logarithmic variables, the solver and the error estimation process will easily see the significance of an error estimate of 10^{-6} in a region where k is of order 10^{-6}, and the mesh will be refined in that region. In other words, logarithmic variables will always detect regions where the error is sizable when compared with the norm of the solution. This is not the case when using k as a dependent variable. This reasoning holds for ϵ and is also applicable to the nonlinear finite element equation solver. In the last case this results in more accurate solution of the discrete equations.

When using k and ϵ as dependent variables, small errors in regions of low-turbulence variables can have disastrous effects on the accuracy of the eddy viscosity. Indeed, because the eddy viscosity is given by

$$\mu_T = \rho C_\mu (k^2/\epsilon)$$

the error in the eddy viscosity can be written as

$$e_{\mu_T} / \mu_T = 2(e_k/k) - (e_\epsilon/\epsilon)$$

which shows that the relative errors in k and ϵ accumulate in that of the eddy viscosity. This means that a 5% uncertainty in k and ϵ results in a 15% error in eddy viscosity. Furthermore, the error in eddy viscosity can be amplified by the division if k and/or ϵ are small. This amplification can have disastrous effects, especially in the freestream of flows over airfoils or in free shear layers. It is straightforward to show that, when logarithmic variables are used, the relationship between the eddy viscosity error and the error in the logarithmic variables is given by

$$e_{\mu_T} = \mu_T (2e_{\mathcal{K}} + e_{\mathcal{E}})$$

This shows that the error estimation in the eddy viscosity will no longer be affected by the local level of the turbulence variables and is no longer subject to the numerical difficulties associated with division by small numbers.

VI. Applications

A. Shear Layer with a Closed-Form Solution

This problem served as a validation case in Ref. 1 to test the accuracy of the error estimation technique. In this flow the eddy viscosity is a linear function of x and is independent of y. The computational domain is the rectangle $[100, 300] \times [-75, 75]$. The problem was solved first in logarithmic variables and then with the standard form of the k–ϵ model. All equations are solved using the GLS formulation.

The meshes generated by the adaptive procedure are shown in Fig. 1. On the last mesh several diagonal bands of refinement can be clearly seen. They correspond to regions of rapid variation in velocity, $\ell n(k)$, $\ell n(\epsilon)$, and μ_T. The same meshes have been used to compute the solution using (k, ϵ) and $(\mathcal{K}, \mathcal{E})$ as dependent variables. In this way, we can compare the accuracy of the eddy viscosity obtained using both approaches. Figure 2 presents the trajectory of the true error for the eddy viscosity. As can be seen, the use of logarithmic variables leads to a far more accurate prediction of the eddy viscosity than the classical solution approach. This fact is illustrated in Fig. 3, which shows the eddy viscosity field obtained on first mesh. The plot on the left illustrates results from the (k, ϵ) solution, whereas the one on the right presents the solution obtained using logarithmic variables. Both plots contain 20 contour lines from 0.1372 to 0.4116. As can be seen, logarithmic variables lead to significant improvements in the quality of the eddy viscosity

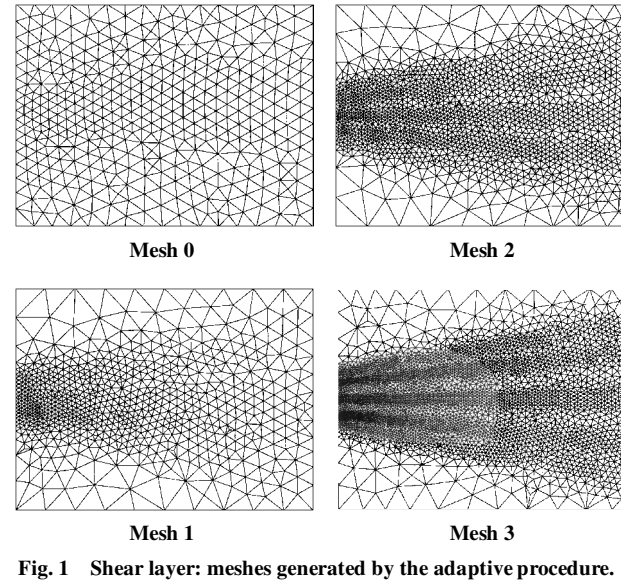

Fig. 1 Shear layer: meshes generated by the adaptive procedure.

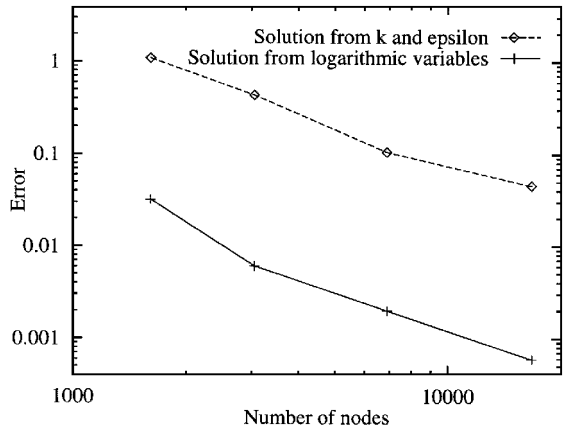

Fig. 2 Trajectory of the true error for the eddy viscosity.

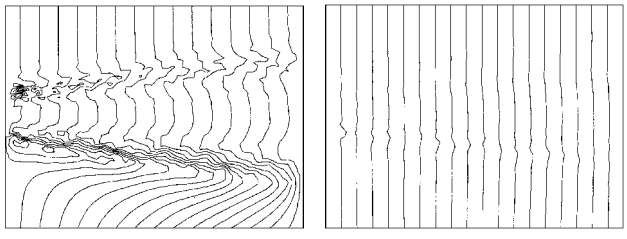

Solution from k and ϵ **Solution from logarithms ($\mathcal{K}$ and $\mathcal{E}$)**

Fig. 3 Contour lines of the turbulent viscosity on the first mesh.

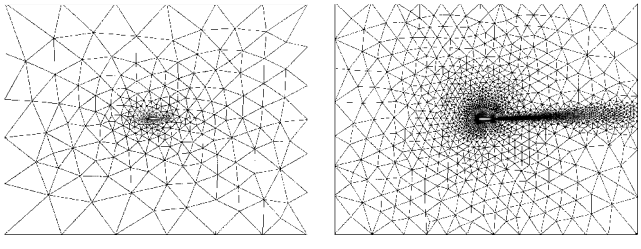

Initial mesh **Final mesh**

Fig. 4 NACA0012, α = 3.59 deg.

distribution. This is mainly due to the fact that a quadratic interpolation of the logarithm of turbulence quantities is more accurate than a quadratic interpolation of the turbulence quantities themselves in regions of rapid variations. Although improvements in the accuracy of the solution are more pronounced on coarser meshes, solutions using logarithmic variables are always more accurate on any mesh than those obtained from the (k, ϵ) calculation.

B. Turbulent Flow over a NACA0012 Airfoil at 3.59 Degrees of Incidence

Incompressible turbulent flow over a NACA0012 airfoil is computed at a Reynolds number of 1.8×10^6. The computational domain is the rectangle $[-10, 11] \times [-8, 8]$ with the airfoil located between $x = 0$ and 1. Logarithmic variables and GLS formulation are used. The initial and final meshes obtained after four cycles of adaptation are shown in Fig. 4. As can be seen, the initial mesh is very coarse, whereas the final mesh is highly refined near the airfoil. Note also the mesh refinement in the wake of the airfoil. Figure 5 illustrates details of the mesh near the airfoil. The extreme clustering of grid points along the airfoil is clearly seen. Figure 6 presents pressure contours obtained on these meshes. The pressure contours are discontinuous because the finite element discretization of the momentum and continuity equations uses discontinuous pressure approximation. In this flow problem, it is known that the pressure is continuous. Hence, the degree of continuity of the pressure contours is a measure of the accuracy of the pressure solution. It is clear from Fig. 6 that the pressure solution improves with mesh adaptation.

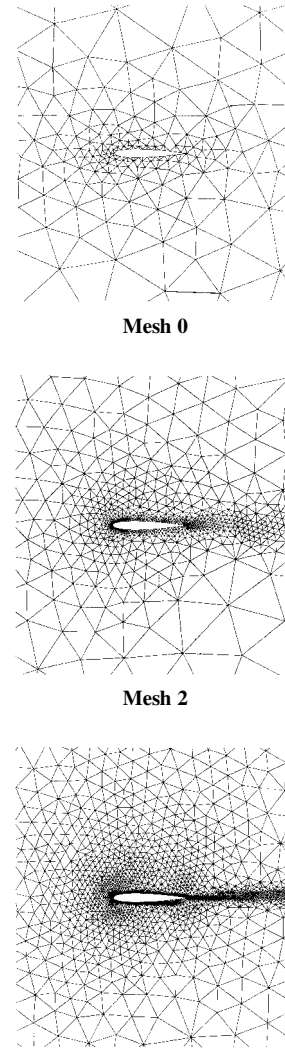

Mesh 0

Mesh 2

Mesh 4

Fig. 5 Details of the adapted meshes near the airfoil.

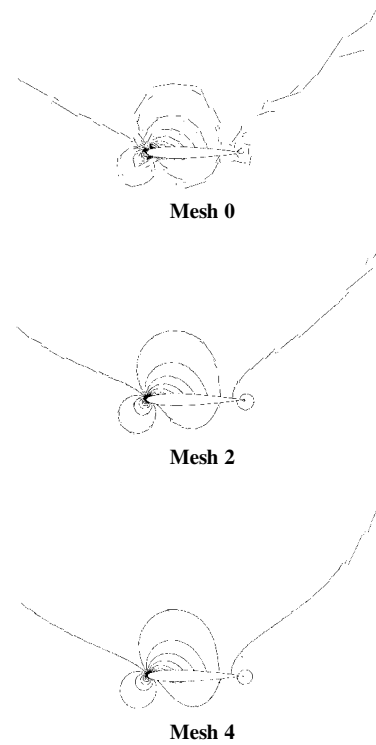

Mesh 0

Mesh 2

Mesh 4

Fig. 6 Contour lines of the pressure.

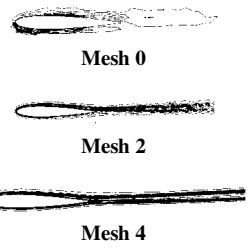

Fig. 7 Contour lines of the eddy viscosity.

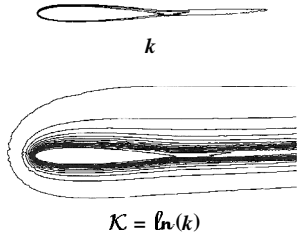

Fig. 8 Contour lines of k and $\ell n(k)$ on the final mesh.

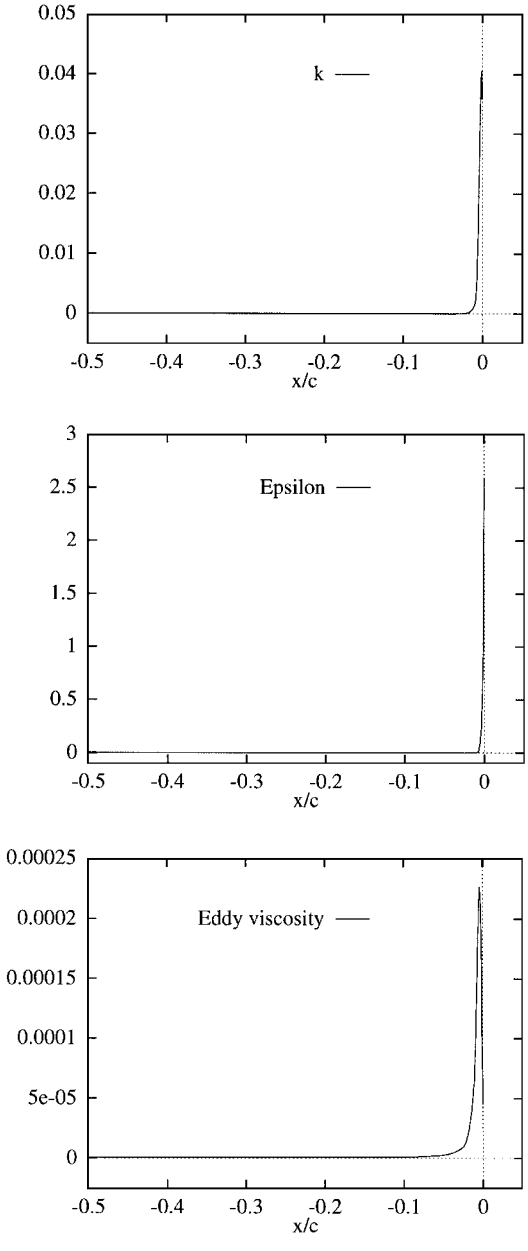

Fig. 9 Variation of turbulence variables on the x axis.

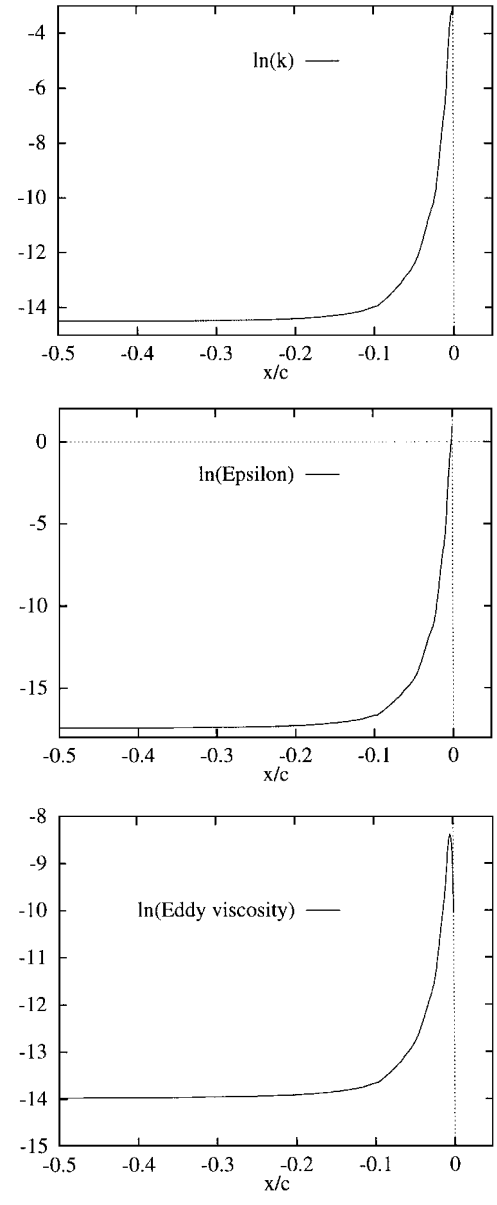

Fig. 10 Variation of logarithmic variables on the x axis.

Figure 7 presents contours of the eddy viscosity obtained on the meshes shown in Fig. 5. Twenty contours are plotted for eddy viscosity values in the range $[7.6 \times 10^{-7},\ 2.2 \times 10^{-4}]$ (results are presented for the dimensionless eddy viscosity computed as $\tilde{\mu}_T = \mu_T/(\rho U_0 L_0)$, where U_0 and L_0 are the reference velocity and length, respectively). Improvement in the resolution of the eddy viscosity field with adaptation is clearly seen. Figure 8 presents contours of k and $\mathcal{K}$ obtained on the final mesh. Similar results are obtained for ϵ and $\mathcal{E}$. Therefore only the results for k are shown. Both plots contain 20 contour lines from 1.97×10^{-7} to 4.28×10^{-2} in the case of k and from -15.44 to -3.15 for the logarithm (values of k are dimensionless and computed as $\tilde{k} = k/U_0^2$). Figure 8 shows the extreme thinness of the fronts of k in the boundary layer. Note that k and ϵ vary by at least six orders of magnitude in the vicinity of the airfoil. The fields of $\mathcal{K}$ and $\mathcal{E}$ present smoother variations than k and ϵ, and hence discretization of logarithms is more accurate; the fronts in $\mathcal{K}$ and $\mathcal{E}$ are not as steep as those in k and ϵ. To better illustrate these observations, Fig. 9 presents the turbulence variable[9] distributions along the x axis upstream of the airfoil leading edge. Similar distributions of logarithmic variables are presented in Fig. 10. As can be seen, the variations of k and ϵ are confined to a very thin and narrow layer near the airfoil. For the same fields of k and ϵ, logarithmic variables show much gentler variations. This is especially true for ϵ, which takes on very large values near the leading-edge stagnation point (dimensionless value of order 2, whereas it is of

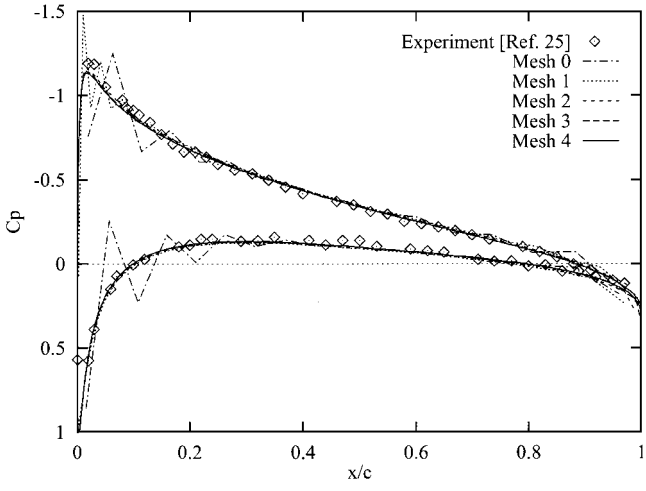

Fig. 11 Pressure coefficient distribution.

order 10^{-8} in the freestream). Note also that close to the leading edge we find points having very small values of ϵ, but for which the eddy viscosity is important. In such a region, even small errors for ϵ may have disastrous effects on the eddy viscosity. This problem is completely eliminated when logarithmic variables are used to compute the solution.

Finally, Fig. 11 presents a comparison of predicted values of the pressure coefficient with experimental measurements.[25] The plots correspond to the different meshes generated by the adaptive procedure. As can be seen, the agreement with the experimental data improves with adaptivity. The agreement is very good for the solution obtained on the final mesh.

VII. Conclusion

This paper has presented a change of dependent variables that guarantees positivity of turbulence variables in the k–ϵ model of turbulence. The use of logarithmic variables for turbulence quantities eliminates the need for clipping or limiting turbulence variables from below in the course of numerical iteration. The use of logarithmic variables presents the following advantages over standard variables.

1) Turbulence quantities are always positive.

2) The eddy viscosity never becomes negative.

3) Solutions can be obtained on coarser initial meshes.

4) Logarithmic variables vary more slowly than k and ϵ; hence, resolution of fronts in turbulence variables and eddy viscosity is improved.

5) Adaptation using error estimates in logarithmic variables leads to significant improvement in accuracy of the solution in regions where turbulence quantities are extremely small.

Numerical experiments have shown that the use of logarithmic variables leads to improved prediction of the eddy viscosity field in problems having an analytical solution and for practical turbulent flows. This is due to the combined effect of improved resolution resulting from the use of logarithmic variables and the elimination of clipping in the solution algorithm.

Acknowledgments

The work of D. Pelletier was supported in part by grants from the National Science and Engineering Research Council and the Fonds de Formation de Chercheurs et d'Aide a la Recherche and by U.S. Air Force Office of Scientific Research Grant F49 620-96-1-0329.

References

[1]Ilinca, F., Pelletier, D., and Garon, A., "An Adaptive Finite Element for a Two-Equation Turbulence Model in Wall Bounded Flows," *International Journal for Numerical Methods in Fluids*, Vol. 24, No. 1, 1997, pp. 101–120.

[2]Ilinca, F., Pelletier, D., and Arnoux-Guisse, F., "Adaptive Remeshing for Turbulent Free Shear Flows," *International Journal for Computational Fluid Dynamics*, Vol. 8, No. 3, 1997, pp. 171–188.

[3]Menter, F. R., "Zonal Two-Equation k–ω Turbulence Models for Aerodynamic Flows," AIAA Paper 93-2906, July 1993.

[4]Yang, Z., and Shih, T. H., "A Gallilean and Tensorial Invariant k–ϵ Model for Near-Wall Turbulence," AIAA Paper 93-3105, July 1993.

[5]Shur, M., Strelets, M., Zaikov, L., Gulyaev, A., Kozlov, V., and Secundov, A., "Comparative Testing of One- and Two-Equation Turbulence Models for Flows with Separation and Reattachment," AIAA Paper 95-0863, Jan. 1995.

[6]Jacon, F., and Knight, D., "A Navier–Stokes Algorithm for Turbulent Flows Using an Unstructured Grid and Flux Difference Splitting," AIAA Paper 94-2293, June 1994.

[7]Spalart, P., and Allmaras, S. R., "A One-Equation Turbulence Model for Aerodynamic Flows," AIAA Paper 92-0439, Jan. 1992.

[8]Baldwin, B. S., and Barth, T. J., "A One-Equation Turbulence Transport Model for High Reynolds Number Wall-Bounded Flows," NASA TM-102847, Aug. 1990.

[9]Launder, B. E., and Spalding, D. B., *Mathematical Models of Turbulence*, 6th ed., Academic, London, 1972.

[10]Pelletier, D., and Ilinca, F., "Adaptive Remeshing for the k–ϵ Model for Turbulence," *AIAA Journal*, Vol. 35, No. 4, 1997, pp. 640–646.

[11]Ilinca, F., Pelletier, D., and Garon, A., "Positivity Preserving Formulations for Adaptive Solution of Two-Equation Models of Turbulence," AIAA Paper 96-2056, June 1996.

[12]Kim, S. E., and Choudhury, D., "Computations of Complex Turbulent Flows and Heat Transfer Using Two-Layer Based Wall Functions," *Proceedings of the 30th National Heat Transfer Conference*, HTD-Vol. 311, American Society of Mechanical Engineers, New York, 1995.

[13]Hughes, T. J. R., Franca, L. P., and Balestra, M., "A New Finite Element Formulation for Computational Fluid Dynamics: V. Circumventing the Babuška-Brezzi Condition: A Stable Petrov-Galerkin Formulation of the Stokes Problem Accommodating Equal-Order Interpolations," *Computer Methods in Applied Mechanics and Engineering*, Vol. 59, 1986, pp. 85–99.

[14]Hughes, T. J. R., Franca, L. P., and Hulbert, G. M., "A New Finite Element Formulation for Computational Fluid Dynamics: VII. The Galerkin-Least-Squares Method for Advective-Diffusive Equations," *Computer Methods in Applied Mechanics and Engineering*, Vol. 73, 1989, pp. 173–189.

[15]Franca, L. P., and Frey, S. L., "Stabilized Finite Element Methods: II. The Incompressible Navier–Stokes Equations," *Computer Methods in Applied Mechanics and Engineering*, Vol. 99, Nos. 2, 3, 1992, pp. 209–233.

[16]Tezduyar, T. E., Aliabadi, S. K., Behr, M., and Mittal, S., "Massively Parallel Finite Element Simulation of Compressible and Incompressible Flows," Army High Performance Computing Reserach Center, Research Rept. 94-013, Minneapolis, MN, Feb. 1994.

[17]Franca, L. P., and Hughes, T. J. R., "Convergence Analyses of Galerkin-Least-Squares Methods for Symmetric Advective-Diffusive Forms of the Stokes and Incompressible Navier–Stokes Equations," *Computer Methods in Applied Mechanics and Engineering*, Vol. 105, No. 2, 1993, pp. 285–298.

[18]Ilinca, F., "Méthodes d'éléments finis adaptatives pour les écoulements turbulents," Ph.D. Thesis, Dept. of Mechanical Engineering, École Polytechnique of Montréal, Montréal, PQ, Canada, March 1996.

[19]Zienkiewicz, O. C., and Zhu, J. Z., "The Superconvergent Patch Recovery and A Posteriori Error Estimators. Part 1: The Recovery Technique," *International Journal for Numerical Methods in Engineering*, Vol. 33, No. 7, 1992, pp. 1331–1364.

[20]Zienkiewicz, O. C., and Zhu, J. Z., "The Superconvergent Patch Recovery and A Posteriori Error Estimators. Part 2: Error Estimates and Adaptivity," *International Journal for Numerical Methods in Engineering*, Vol. 33, No. 7, 1992, pp. 1365–1382.

[21]Pelletier, D., Garon, A., and Ilinca, F., "Adaptive Finite Element Algorithms for the k–ϵ and k–ω Models of Turbulence," *Advances in Finite Element Analysis in Fluid Dynamics*, Proceedings of the ASME Winter Annual Meeting, American Society of Mechanical Engineers, New York, 1994.

[22]Ignat, L., Pelletier, D., and Ilinca, F., "An Adaptive Finite Element Method for Turbulent Heat Transfer," AIAA Paper 96-0607, Jan. 1996.

[23]Ilinca, F., and Pelletier, D., "A Pressure Based Adaptive Finite Element Algorithm for Compressible Viscous Flows," AIAA Paper 96-0679, Jan. 1996.

[24]Peraire, J., Vahdati, M., Morgan, K., and Zienkiewicz, O. C., "Adaptive Remeshing for Compressible Flow Computations," *Journal of Computational Physics*, Vol. 72, No. 2, 1987, pp. 26–37.

[25]"Experimental Data Base for Computer Program Assessment," AGARD Advisory Rept. 138, 1979.

F. W. Chambers
Associate Editor